ORNL/TM-9801

OAK RIDGE NATIONAL LABORATORY

MARTIN MARIETTA

Neutron-Photon Multigroup Cross Sections for Neutron Energies ≤400 MeV (Revision 1)

R. G. Alsmiller, Jr.
J. M. Barnes
J.D. Drischler

OPERATED BY
MARTIN MARIETTA ENERGY SYSTEMS, INC.
FOR THE UNITED STATES
DEPARTMENT OF ENERGY

Printed in the United States of America. Available from
National Technical Information Service
U.S. Department of Commerce
5285 Port Royal Road, Springfield, Virginia 22161
NTIS price codes—Printed Copy: A03; Microfiche A01

ORNL/TM-9801

Engineering Physics and Mathematics Division

NEUTRON-PHOTON MULTIGROUP CROSS SECTIONS FOR NEUTRON ENERGIES ≤400 MeV (Revision 1)*

R. G. Alsmiller, Jr.
J. M. Barnes+
J. D. Drischler

*Submitted for Journal publication
+Computing & Telecommunications

Date Published - February 1986

Research sponsored by
Office of High Energy
and Nuclear Physics
U.S. Department of Energy

Prepared by the
Oak Ridge National Laboratory
Oak Ridge, Tennessee 37831
operated by
Martin Marietta Energy Systems, Inc.
for the
U.S. DEPARTMENT OF ENERGY
under Contract No. DE-AC05-840R21400

TABLE OF CONTENTS

Abstract

Multigroup cross sections (66 neutron groups and 22 photon groups) are described for neutron energies from thermal to 400 MeV. The elements considered are hydrogen, ^{10}B, ^{11}B, carbon, nitrogen, oxygen, sodium, magnesium, aluminum, silicon, sulfur, potassium, calcium, chromium, iron, nickel, tungsten, and lead. The cross section data presented are a revision of similar data presented previously. In the case of iron, transport calculations using the earlier and the revised cross sections are presented and compared, and significant differences are found. The revised cross sections are available from the Radiation Shielding Information Center of the Oak Ridge National Laboratory.

I. INTRODUCTION

For a variety of applications, e.g., accelerator shielding design,[1] neutron radiotherapy,[2] radiation damage studies,[3] etc., it is necessary to carry out transport calculations involving medium-energy (≥20 MeV) neutrons. In a previous paper[4] (see also Ref. 5), neutron-photon multigroup cross sections in the ANISN[6] format for neutrons from thermal to 400 MeV were presented. In the present paper the cross section data presented previously have been revised to make them agree with available experimental data.

The elements considered (hydrogen, ^{10}B, ^{11}B, carbon, nitrogen, oxygen, sodium, magnesium, aluminum, silicon, sulfur, potassium, calcium, chromium, iron, nickel, tungsten, and lead) and the basic approximations used in developing the revised cross sections are the same as those used in Ref. 4. There are, however, two substantive differences between the data presented here and those given previously. First, except for sulfur and lead, the revised cross sections at neutron energies below 19.6 MeV are based on ENDF/B-V[7] and on a P_5 Legendre expansion, while those in Ref. 4 below 14.9 MeV were based on ENDF/B-IV and used a P_3 Legendre expansion. Second, the elastic cross sections used here at neutron energies ≥19.6 MeV have been chosen so that the total, i.e., elastic + nonelastic, cross sections agree with experimental data. The elastic cross sections used previously were based on optical model calculations with global parameters and, as pointed out by V. Herrnberger,[8] this led to total cross sections that were not always in good agreement with experimental data.

In Section II the procedures used to generate the cross sections are discussed and some cross section data are presented. In Section III the results of transport calculations for an iron shield using the data from Ref. 4 and those presented here are compared.

The multigroup cross section data described here are available from the Radiation Shielding Information Center of the Oak Ridge National Laboratory.

II. CROSS SECTION CALCULATIONS

A. Neutron Energies ≤19.6 MeV

The multigroup cross sections at neutron energies below 19.6 MeV were, except for the elements sulfur and lead, obtained by collapsing the 174-neutron, 38-photon VITAMIN-E data library[9] that is based on ENDF/B-V. For the elements sulfur and lead, the cross sections at neutron energies ≤19.6 MeV are the same as those in Ref. 4 and are therefore more approximate than the cross sections for the other elements considered here.

The fine-group library was collapsed with ANISN[6] using a spherical configuration, a source characteristic of a fusion reactor spectrum as specified by R. T. Santoro et al.,[10] weighting functions as specified by R. T. Santoro et al.,[11] a symmetric S_{12} angular quadrature, and a P_5 Legendre expansion of the cross sections.

The energy group boundaries of the multigroup cross sections are shown in Table 1. The neutron energy group boundaries below 14.9 MeV are the same as those used in Ref. 4. The photon energy group boundaries are also the same as those in Ref. 4, except that a group has been added above 14 MeV.

Table 1

Energy Group Structure

Upper Group Energy (MeV)							
Neutron Groups						Photon Groups	
400	140	45	12.2	1.35	7.10×10^{-3}	20.0	4.50
375	120	40	10.0	1.11	3.35×10^{-3}	14.0	4.00
350	110	35	8.19	9.07×10^{-1}	1.58×10^{-3}	12.0	3.50
325	100	30	6.70	7.43×10^{-1}	4.54×10^{-4}	10.0	3.00
300	90	27.5	5.49	4.98×10^{-1}	1.01×10^{-4}	8.00	2.50
275	80	25.0	4.49	3.34×10^{-1}	2.26×10^{-5}	7.50	2.00
250	70	22.5	3.68	2.24×10^{-1}	1.07×10^{-5}	7.00	1.50
225	65	19.6	3.01	1.50×10^{-1}	5.04×10^{-6}	6.50	1.00
200	60	17.5	2.46	8.65×10^{-2}	2.38×10^{-6}	6.00	4.00×10^{-1}
180	55	14.9	2.02	3.18×10^{-2}	1.12×10^{-6}	5.50	2.00×10^{-1}
160	50	13.5	1.65	1.50×10^{-2}	4.14×10^{-7}[a]	5.00	1.00×10^{-1}[b]

[a]The lower energy of this group is 1.00×10^{-10} MeV.
[b]The lower energy of this group is 1.00×10^{-2} MeV.

B. Neutron Energies ⩾19.6 MeV

At neutron energies ⩾19.6 MeV, the multigroup cross sections described here are based on intranuclear cascade and optical model calculations as in Ref. 4, supplemented by experimental data. As explained below, many of the data used here are the same as those used in Ref. 4.

In Ref. 4 photon production from neutron-nucleus nonelastic collisions at neutron energies ⩾14.9 MeV was neglected and similarly here for all elements considered photon production from neutron-nucleus collisions at energies ⩾19.6 MeV is neglected. Some information on the validity of this approximation is given in Ref. 12.

For the elements hydrogen, ^{10}B, ^{11}B, sulfur, potassium, calcium, chromium, and tungsten the multigroup cross section data presented here are the same as those in Ref. 4.

For all other elements considered here, except lead, the neutron-nucleus nonelastic cross sections and the energy-angle distributions of neutrons from neutron-nucleus nonelastic collisions are the same as those used in Ref. 4. Also, for these elements the energy-angle distributions of neutrons from elastic scattering at energies ⩾19.6 MeV are taken to be the same as those in Ref. 4.

With these specifications the only quantity that remains to be determined is the elastic scattering cross section as a function of energy. This cross section has been determined by adjusting it to make the total cross section agree with experimental data.

In Fig. 1 the total cross sections used in compiling the multigroup cross sections presented here (solid curve) are compared with experimental data.[13-25] References to the various experimental data are given in the figure caption. It should be noted that in Fig. 1 only experimental data at energies ⩾50 MeV are shown. This is not because of the absence of data points but rather because of the very large number of available data points make it impractical to reproduce them here. References and graphs of much of the data available in the 20 to 50 MeV energy range are given in Ref. 26. The value of the total cross section at an energy of 19.6 MeV for each of the elements shown in Fig. 1 is taken from ENDF/B-V.[7] The purpose of Fig. 1 is to indicate the extent to which the solid curve is determined by available experimental data at energies ⩾50 MeV. For some elements, e.g., Fe, the total cross section is rather well defined by the experimental points while in other cases, e.g., Ni, the total cross section is not at all well defined by the experimental data.

For lead, elastic scattering at energies ⩾19.6 MeV is neglected. There are, however, some data available on the nonelastic cross section as a function of energy and these data have been used. In Fig. 2 the solid curves show the neutron-nucleus nonelastic collision cross sections used in the compilation and the points indicate the experimental data.[27,28] In this case, experimental data in the 20 to 50 MeV energy range have also been shown.

Finally, in Table 2 the elastic and nonelastic cross sections that have been used in the compilation are given as a function of energy.

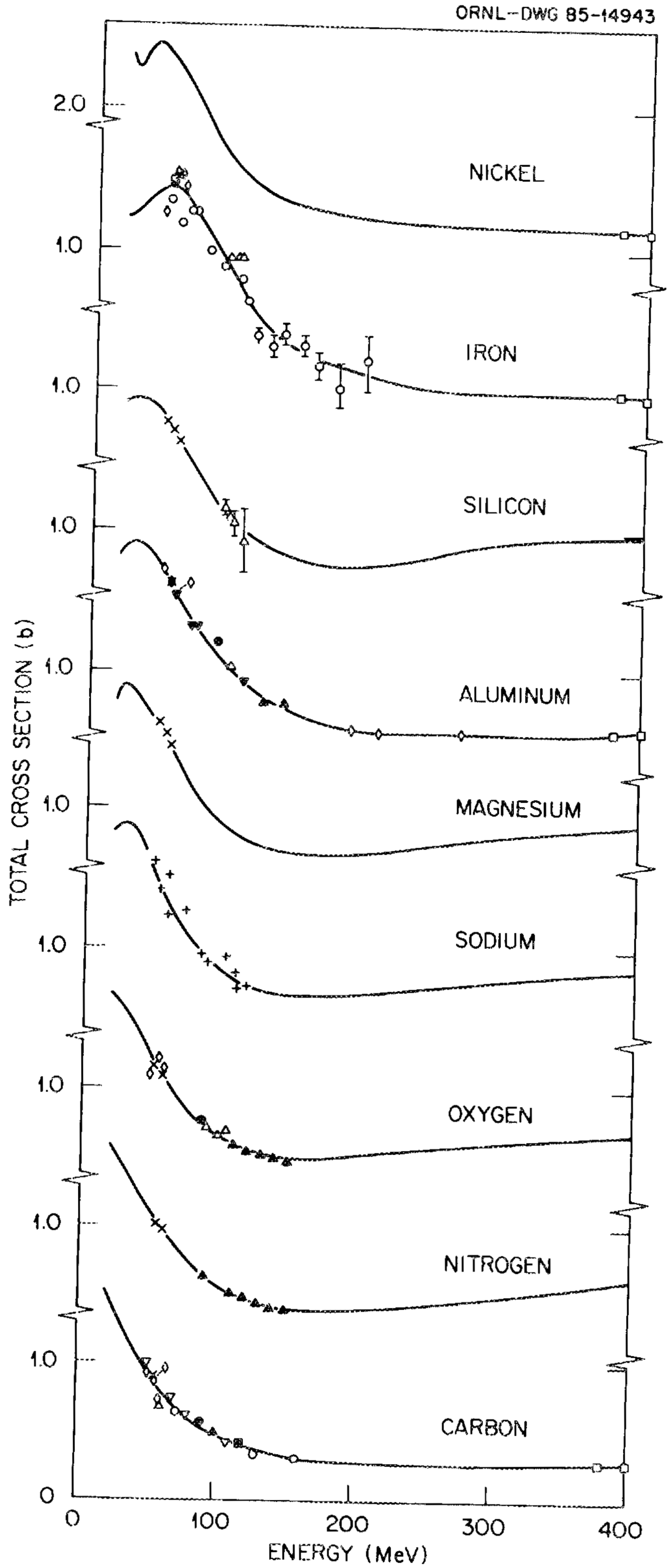

Fig. 1. Total cross sections vs. incident neutron energy for several elements. Here ◊ = Ref. 13, * = Ref. 14, x = Ref. 15, □ = Ref. 16, ■ = Ref. 17, + = Ref. 18, ▲ = Ref. 19, ▼ = Ref. 20, ▽ = Ref. 21, △ = Ref. 22, ● = Ref. 23, ○ = Ref. 24, ◆ = Ref. 25.

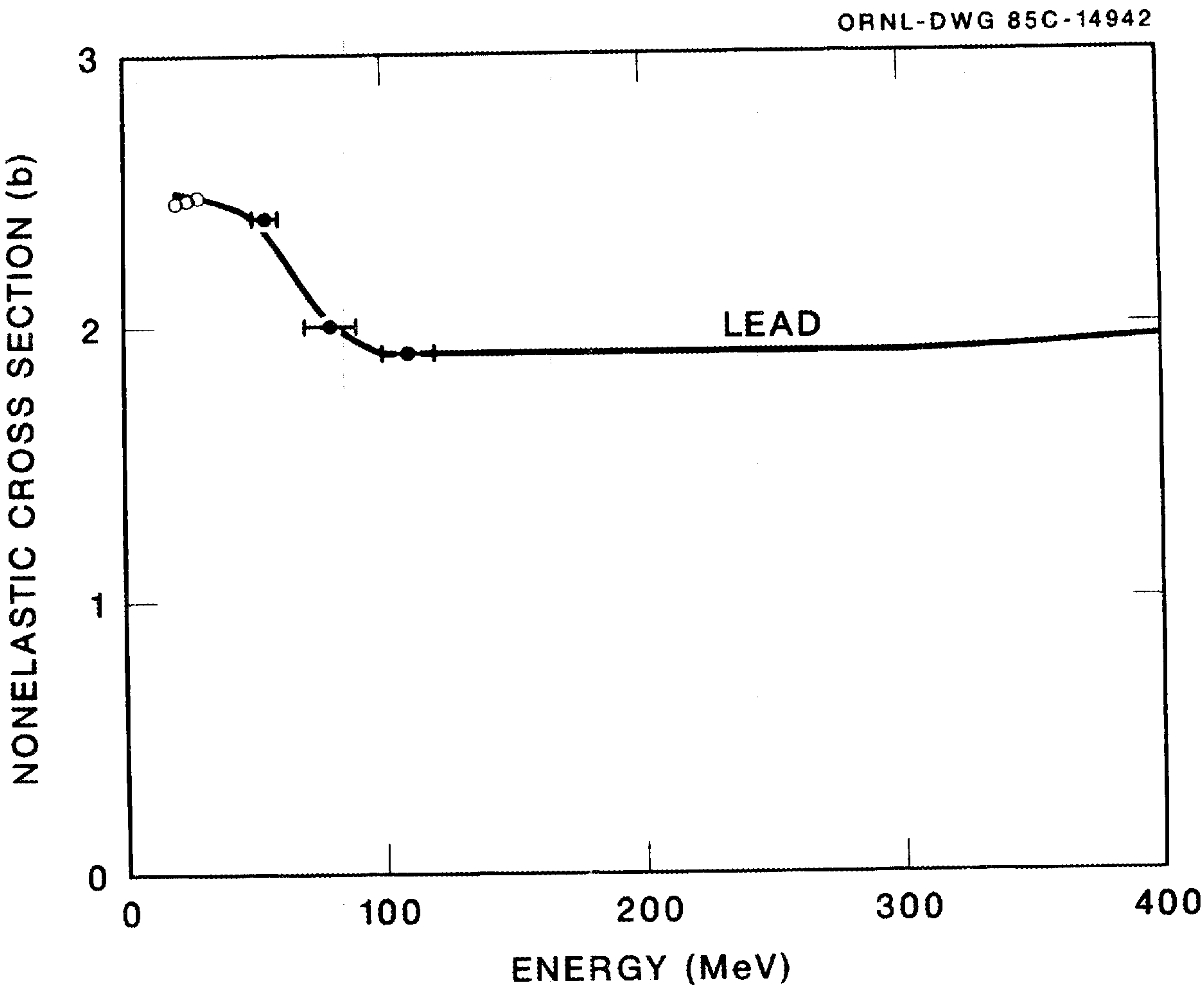

Fig. 2. Nonelastic cross section in lead vs. neutron energy. Here ○ = Ref. 27 and ● = Ref. 28.

Table 2

Elastic and Nonelastic Neutron-Nucleus Cross Sections in Barns as a Function of Energy

Element	Energy (MeV)						
	19.6	**30**	**50**	**100**	**200**	**300**	**400**
^{10}B	0.96[a]	0.88	0.63	0.22	0.16	0.23	0.31
	0.43	0.38	0.32	0.24	0.20	0.19	0.20
^{11}B	0.86	0.85	0.64	0.22	0.18	0.26	0.32
	0.46	0.40	0.34	0.25	0.21	0.20	0.22
Carbon	1.03	0.84	0.59	0.24	0.07	0.06	0.08
	0.50	0.45	0.36	0.24	0.22	0.22	0.22
Nitrogen	0.98	0.98	0.70	0.28	0.15	0.27	0.38
	0.63	0.46	0.39	0.29	0.25	0.24	0.25
Oxygen	1.05	1.06	0.80	0.32	0.24	0.33	0.41
	0.61	0.50	0.42	0.33	0.28	0.27	0.28
Sodium	0.99	1.19	1.03	0.40	0.32	0.43	0.52
	0.86	0.69	0.51	0.41	0.35	0.35	0.35
Magnesium	0.95	1.21	1.08	0.43	0.33	0.44	0.53
	0.82	0.64	0.52	0.42	0.36	0.36	0.36
Aluminum	0.82	1.22	1.20	0.57	0.14	0.15	0.18
	0.97	0.72	0.52	0.43	0.42	0.41	0.41
Silicon	0.93	1.16	1.18	0.57	0.37	0.49	0.58
	0.97	0.78	0.59	0.47	0.40	0.42	0.41
Sulfur	1.00	1.26	1.22	0.54	0.41	0.54	0.64
	0.93	0.78	0.63	0.51	0.44	0.45	0.44
Potassium	0.97	1.24	1.31	0.61	0.48	0.62	0.72
	0.98	0.78	0.69	0.57	0.50	0.50	0.50
Calcium	0.90	1.32	1.32	0.63	0.49	0.63	0.73
	1.18	0.98	0.75	0.58	0.51	0.52	0.51
Chromium	0.78	1.25	1.38	0.73	0.61	0.76	0.87
	1.26	1.10	0.71	0.71	0.64	0.64	0.63
Iron	0.97	1.34	1.58	1.07	0.46	0.34	0.25
	1.28	0.96	0.86	0.73	0.66	0.66	0.75
Nickel	1.04	1.25	1.41	0.81	0.57	0.50	0.44
	1.35	1.25	0.94	0.74	0.68	0.68	0.68
Tungsten	2.52[b]	1.95	1.70	1.53	1.45	1.50	1.48
Lead	2.50[b]	2.48	2.40	1.90	1.90	1.90	1.95

[a]For each element the elastic cross section is given on the first line and the nonelastic cross section is given on the second line.
[b]Elastic scattering at energies $\geqslant$ 19.6 MeV is neglected for tungsten and lead.

C. Multigroup Cross Sections

With the specifications given in Sections II.A and II.B, multigroup cross sections in the form needed for use in the discrete ordinates codes ANISN[6] and DOT[29] and in the MORSE[30] Monte Carlo code may be calculated in a straightforward manner. A weighting function of "1/E" has somewhat arbitrarily been used for neutron energies $\geqslant$ 19.6 MeV.

III. TRANSPORT CALCULATIONS

In Ref. 8 V. Herrnberger proposed a "benchmark" configuration that may be used for the intercomparison of cross section libraries and computational methods. Here this configuration has been used to compare transport results obtained with the original iron cross sections of Ref. 4 and the revised iron cross sections presented here. The original iron cross sections will hereinafter be referred to as HILO, while the revised iron cross sections will be referred to as HILO(R1).

Briefly, the benchmark configuration is that of an iron sphere of radius 5 m with a spherical volumetric isotropic neutron source at its center. The neutron source has a radius of 5 cm and the neutron energy spectrum is uniform over the energy interval 300 to 400 MeV. The density of iron was taken to be 7.84 g/cm^3.

Calculations for this configuration were carried out using the discrete ordinates code ANISN[6] and an S_{12} angular quadrature. In the HILO(R1) calculations a P_5 Legendre expansion was used at all energies while in the HILO calculations a P_5 expansion was used at energies $\geqslant$14.9 MeV and a P_3 expansion was used below this energy. In the HILO library only a P_3 expansion is available below 14.9 MeV.

In Figs. 3 and 4 the neutron flux per unit energy and the photon flux per unit energy are shown at various radii in the iron sphere. In Figs. 3 and 4 and in the remainder of this section all of the transport results are normalized to 1 source neutron per second entering the system. In both Fig. 3 and Fig. 4 there are noticeable differences in the fluxes obtained with the original (HILO) and the revised (HILO(R1)) cross sections.

The total scalar neutron and photon flux, i.e., the result of integrating over energy the fluxes per unit energy in Figs. 3 and 4, are shown as a function of radius in Fig. 5. At the larger radii the neutron and photon scalar fluxes from the HILO(R1) cross sections are significantly larger than the fluxes from the original HILO cross sections. The sharp decreases in the scalar fluxes just before the radius of 500 cm are due to the fact that the shield thickness is 500 cm and thus the albedo contributions to the fluxes are absent.

The two cross section sets were also used to calculate, as a function of radius, the absorbed dose and dose equivalent for neutrons and photons. The neutron fluxes were converted to absorbed doses and dose equivalents with the conversion factors recommended by the International Commission on Radiological Protection.[31] The photon fluxes were converted to doses with the conversion factors recommended by the American Nuclear Standards Institute.[32]

ORNL-DWG 86-7111

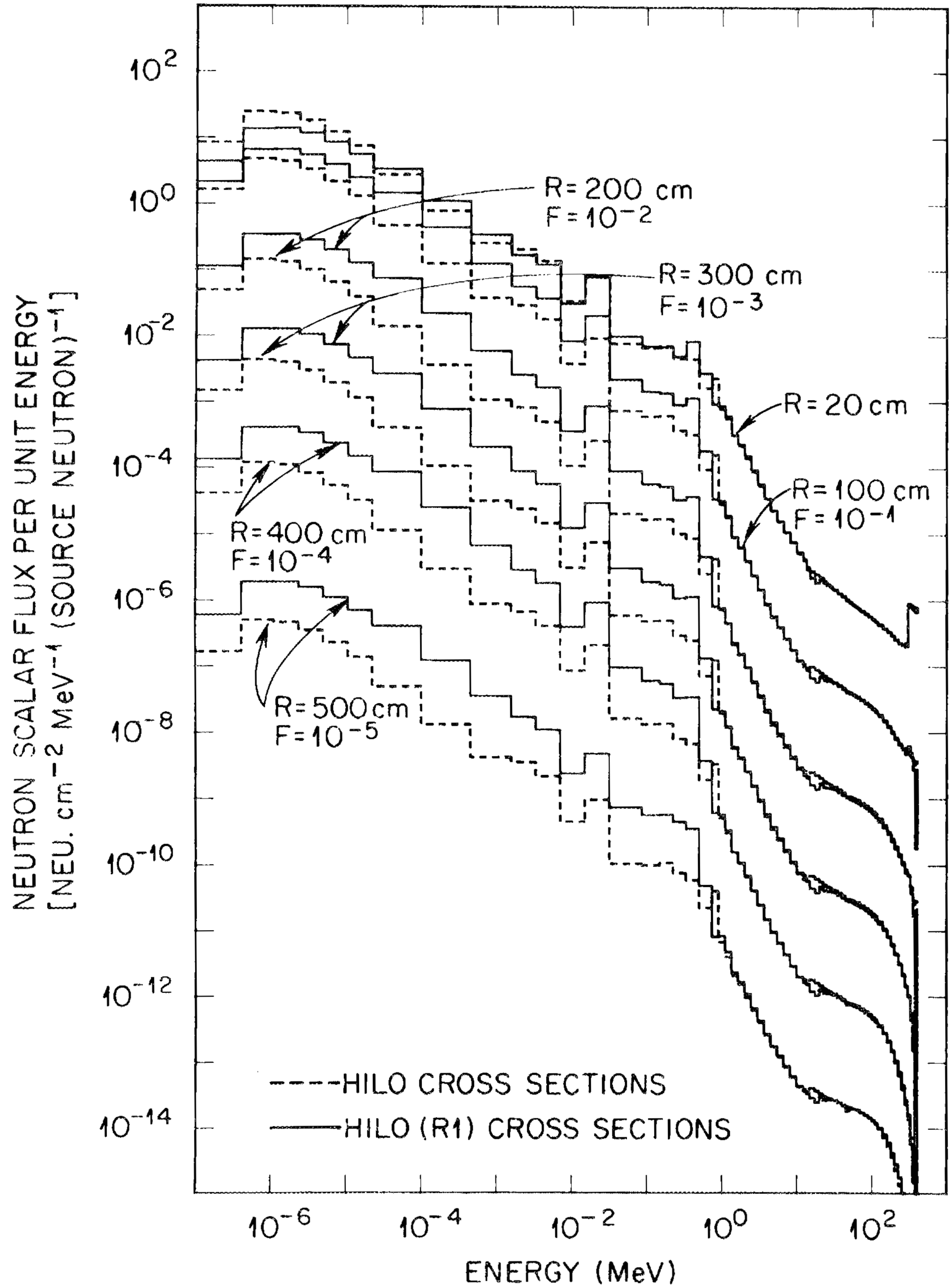

Fig. 3. Neutron flux per unit energy vs. energy at various radii. The factor F associated with various fluxes in the figure is a scale factor used for plotting purposes. The values plotted must be multiplied by the corresponding F to be correctly normalized.

ORNL–DWG 86-7109

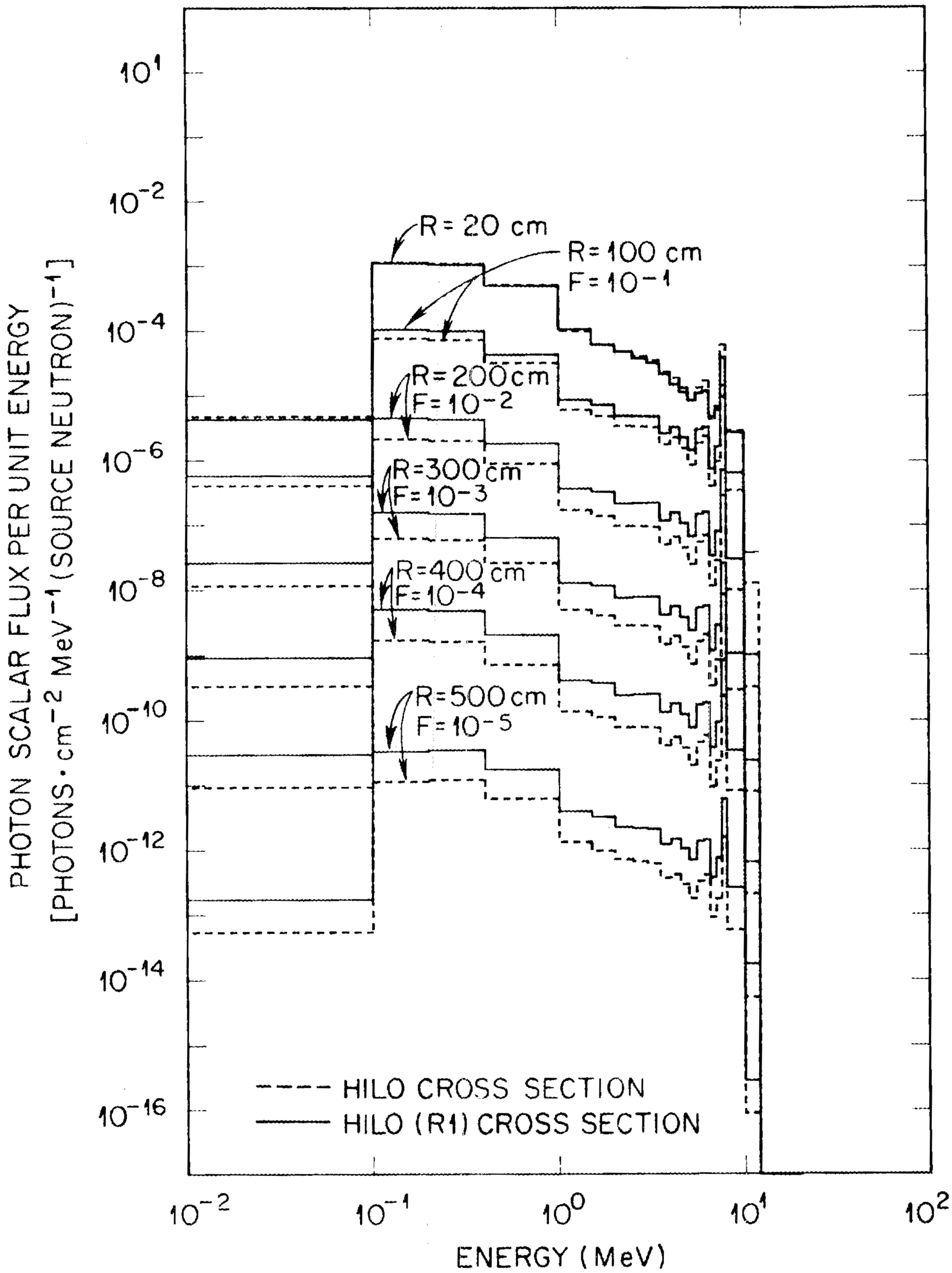

Fig. 4. Photon flux per unit energy vs. energy at various radii. The factor F associated with the various fluxes in the figure is a scale factor used for plotting purposes. The values plotted must be multiplied by the corresponding F to be correctly normalized.

ORNL-DWG 86-7110

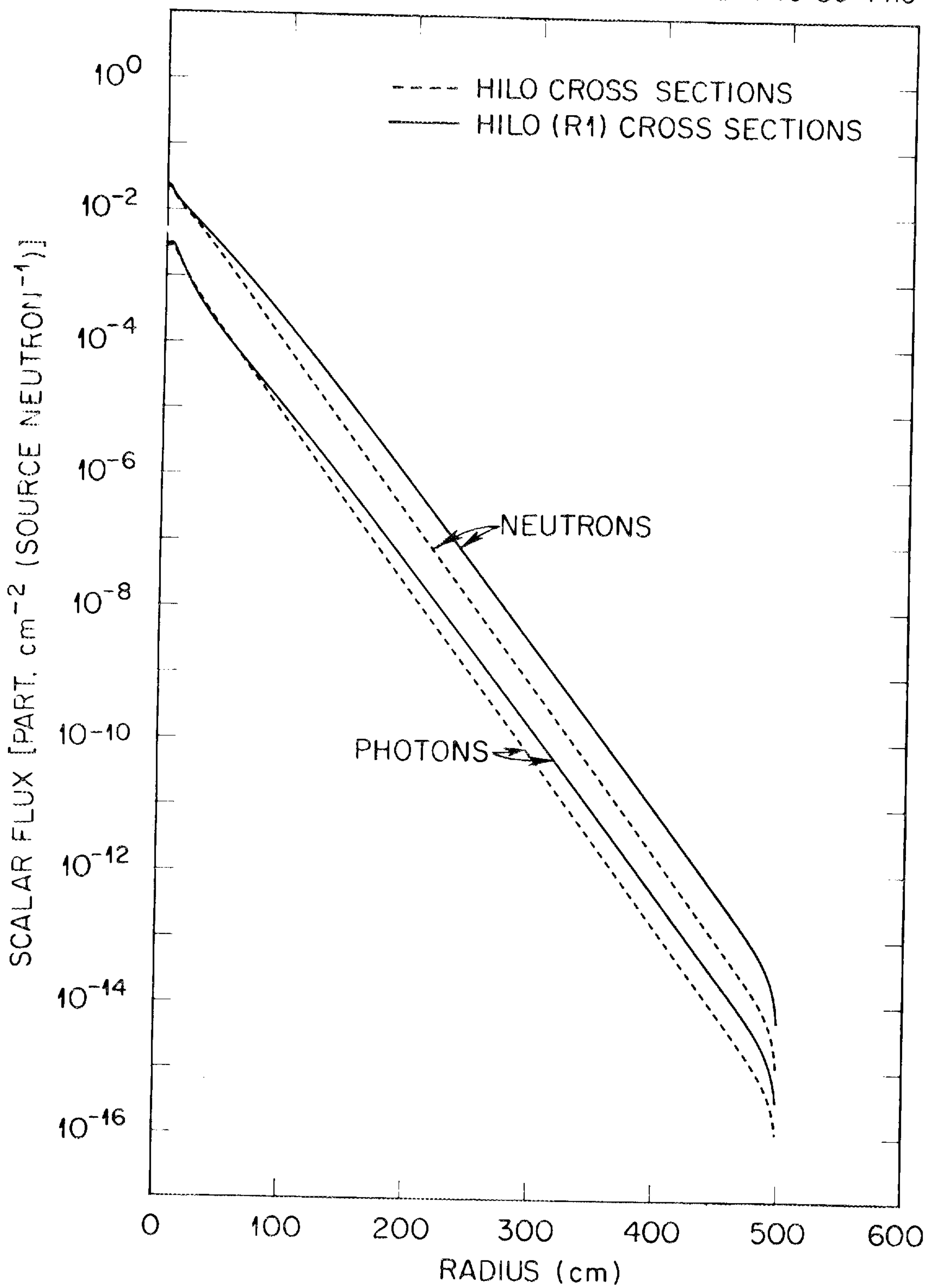

Fig. 5. Scalar neutron and photon fluxes vs. radius.

The results of the dose calculations are given in Table 3. For both neutrons and photons the absorbed doses and dose equivalents from HILO(R1) are larger than those from HILO at the larger radii.

IV. SUMMARY

The HILO neutron-photon cross section library has been revised by modifying the elastic cross section so the total cross section is in agreement with experimental data. The revised cross sections HILO(R1) should be more accurate and are therefore recommended.

Table 3

Comparison of Calculated Absorbed Dose and Dose Equivalent Results in Iron Obtained Using the HILO(R1) and HILO Cross Section Libraries

(The first line in the table for each radius is from HILO(R1) and the second line is from HILO.)

Radius (cm)	Absorbed Dose Due to Neutrons $\left(\frac{\text{mrad/hr}}{\text{(source neu./sec.)}}\right)$	Absorbed Dose Due to Photons $\left(\frac{\text{mrad/hr}}{\text{(source neu./sec.)}}\right)$	Dose Equivalent Due to Neutrons $\left(\frac{\text{mrem/hr}}{\text{(source neu./sec.)}}\right)$	Dose Equivalent Due to Photons $\left(\frac{\text{mrem/hr}}{\text{(source neu./sec.)}}\right)$
20	5.0×10^{-5}	1.4×10^{-6}	3.7×10^{-4}	1.4×10^{-6}
	4.6×10^{-5}	1.5×10^{-6}	3.3×10^{-4}	1.5×10^{-6}
60	4.8×10^{-6}	1.5×10^{-7}	3.3×10^{-5}	1.5×10^{-7}
	3.2×10^{-6}	1.5×10^{-7}	2.2×10^{-5}	1.5×10^{-7}
100	5.5×10^{-7}	2.1×10^{-8}	33.4×10^{-6}	2.1×10^{-8}
	2.8×10^{-7}	14×10^{-8}	1.8×10^{-6}	1.4×10^{-8}
200	2.1×10^{-9}	9.8×10^{-11}	1.2×10^{-8}	9.8×10^{-11}
	7.5×10^{-10}	4.1×10^{-11}	4.8×10^{-9}	4.1×10^{-11}
300	7.0×10^{-12}	3.5×10^{-13}	3.7×10^{-11}	3.5×10^{-13}
	2.1×10^{-12}	1.2×10^{-13}	1.4×10^{-11}	1.2×10^{-13}
400	2.2×10^{-14}	1.1×10^{-15}	1.1×10^{-13}	1.1×10^{-15}
	5.8×10^{-15}	3.3×10^{-16}	3.7×10^{-14}	3.3×10^{-16}
450	1.2×10^{-15}	6.1×10^{-17}	6.2×10^{-15}	6.1×10^{-17}
	3.0×10^{-16}	1.7×10^{-17}	1.9×10^{-15}	1.7×10^{-17}
500	1.2×10^{-17}	6.3×10^{-19}	8.3×10^{-17}	6.3×10^{-19}
	3.8×10^{-18}	1.8×10^{-19}	2.8×10^{-17}	1.8×10^{-19}

REFERENCES

1. R. G. Alsmiller, Jr., J. Barish, and R. L. Childs, "Skyshine at Neutron Energies ≤400 MeV," *Particle Accel.* **11**, 131 (1981).

2. Proc. Second Symp. Neutrons Dosimetry in Biology and Medicine, Neuherberg 1, Munich, Germany, Sept. 30-Oct. 4, 1974, G. Berger and H. B. Ebert, Eds., EUR-5273 d-e-f, Commission of the European Communities (March, 1975).

3. "Conceptual Design Study for Fusion Materials Irradiation Test Facility," TL-961, Hanford Engineering Development Laboratory (1977).

4. R. G. Alsmiller, Jr. and J. Barish, "Neutron-Photon Multigroup Cross Sections for Neutron Energies ≤400 MeV," *Nucl. Sci. Eng.* **80**, 448 (1982).

5. R. G. Alsmiller, Jr. and J. Barish, "Neutron-Photon Multigroup Cross Sections for Neutron Energies ≤60 MeV," *Nucl. Sci. Eng.* **69**, 378 (1979).

6. W. W. Engle, Jr., "A User's Manual for ANISN, A One-Dimensional Discrete Ordinates Transport Code with Anisotropic Scattering," K-1693, Oak Ridge Gaseous Diffusion Plant (1967).

7. R. Kinsey, "ENDF/B Summary Documentation," National Nuclear Data Center, Brookhaven National Laboratory, BNL-NCS-17541 (1979).

8. V. Herrnberger, "Analysis of the High-Energy Neutron Shielding Benchmark," TM-22-82-54, Swiss Federal Institute for Reactor Research (1982).

9. C. R. Weisbin, R. W. Roussin, J. J. Wagschal, J. J. Wagschal, J. E. White, and R. Q. Wright, "VITAMIN-E: An ENDF/B-V Multigroup Cross Section Library for LMFBR Core and Shield, LWR Shield, Dosimetry, and Fusion Blanket Technology," ORNL-5505, Oak Ridge National Laboratory (1979).

10. R. T. Santoro, J. M. Barnes, R. G. Alsmiller, Jr., and J. D. Drischler, "Monte Carlo and Discrete Ordinates Calculations of 14-MeV Neutron Streaming Through a Stainless Steel Duct: Comparison with Experiment I," ORNL/TM-9541, Oak Ridge National Laboratory (1985). (Submitted for publication in Nuclear Science & Engineering)

11. R. T. Santoro, R. W. Roussin, J. M. Barnes, "Flung: Coupled 35-Group Neutron and 21-Group Gamma Ray P_3 Cross Sections for Fusion Applications," Oak Ridge National Laboratory, ORNL/TM-7828 (1981).

12. R. W. Roussin, R. G. Alsmiller, Jr., and J. Barish, "Calculations of the Transport of Neutrons and Secondary Gamma Rays Through Concrete for Incident Neutrons in the Energy Range 15 to 75 MeV," *Nucl. Eng. & Design* **25**, 250 (1973).

13. D. C. Larson, J. A. Harvey and N. W. Hill, "Neutron Cross Sections of Hydrogen, Carbon, Oxygen, and Iron from 500 keV to 60 MeV," Proc. International Conference on Nuclear Cross Sections for Technology, Knoxville, Tennessee, October 22-26, 1979, NBS Special Publication 594, U. S. National Bureau of Standards (1980).

14. C. I. Zanelli et al., (University of California, Davis, CA) "Measurements of Neutron Total and Total Nonelastic Cross Sections for C, O, Ca, and Fe at UC Davis," *Bull. Am. Phys. Soc.* **24**, 658 (1979).

15. M. Auman et al., (University of California, Davis, CA) "Neutron Total Cross Sections of the Light Elements in the Energy Range 24-60 MeV," *Phys. Rev. C* **5**, 1 (1972).

16. W. Schimmerling et al., (Princeton University, Princeton, NJ) "Neutron-Nucleus Total Cross Sections from 900 to 2600 MeV/c," *Phys. Letts.* **37**, 177 (1971).

17. P. Stoler et al., (Rensselaer Polytechnic Institute, Troy, NY) Total Neutron Cross Sections of Capture and Na from En = 1 MeV to 10 MeV," *Bull. Am. Phys. Soc.* **15**, 1688 (1970).

18. A. Langsford et al., (AERE, Harwell, Berkshire, England) "High Resolution Neutron Time-of-Flight Measurements on Na and C from 0.2 to 140 MeV," (Book) Nuclear Structure Study with Neutrons; Proceedings of the International Conference on the Study of Nuclear Structure with Neutrons, Antwerp, Belgium, July 19-23, 1965, 529, p. 65.

19. D. F. Measday (Harvard University, Cambridge, MA) and J. N. Palmieri, "Neutron Total Cross Sections in the Energy Range 80 to 150 MeV," *Nucl. Phys.* **85**, 129 (1965).

20. P. H. Bowen et al., (AERE, Harwell, Berkshire, England) "Neutron Total Cross Sections in the Energy Range 15 to 120 MeV," *Nucl. Phys.* **22**, 640 (1961).

21. T. Coor et al., (Brookhaven National Laboratory, Upton, NY) Nuclear Cross Sections for 1.4-BeV Neutrons," *Phys. Rev.* **98**, 1369 (1955).

22. V. Culler (Harvard University, Cambridge, MA) "Total Cross Sections for High Energy Neutrons," *Phys. Rev* **99**, No. 3, 740 (1955).

23. P. Hillman et al., (Harvard University, Cambridge, MA) "Total Cross Sections of Liquefied Gases for High-Energy Neutrons," *Phys. Rev* **96**, 115 (1954).

24. R. Ragent et al., (University of California, Lawrence Berkeley Laboratory) "The Variation of High-Energy Total Neutron Cross Sections with Energy," (Thesis) UCRL-2337 (1953).

25. J. De Juren (University of California, Lawrence Berkeley Laboratory) and B. J. Mover, "Variation with Energy of Nuclear Collision Cross Sections for High Energy Neutrons," *Phys. Rev* **81**, 919 (1951).

26. D. J. Garber and R. R. Kinsey, "Neutron Cross Sections Volume II, Curves," Brookhaven National Laboratory, BNL-325 (1976).

27. M. H. MacGregor, W. P. Ball, and R. Booth, "Neutron Nonelastic Cross Sections at 21.0, 25.5, and 29.2 MeV," *Phys. Rev* **111**, 1155 (1958).

28. R. G. P. Voss and R. Wilson, "Neutron Inelastic Cross Sections Between 55 and 140 MeV" *Proceedings of the Physical Society (London) (Part A)* **236**, 41 (1956).

29. W. A. Rhoades and R. L. Childs, "An Updated Version of the DOT IV One- and Two-Dimensional Neutron/Photon Transport Code," ORNL-5851, Oak Ridge National Laboratory (1982).

30. M. B. Emmett, "The MORSE Monte Carlo Radiation Transport System," ORNL-4972, Oak Ridge National Laboratory (1975).

31. Recommendations of the International Commission on Radiological Protection, "Protection Against Ionizing Radiation from External Sources," ICRP Publications 21 (1971). (Published by Pergamon Press).

32. American National Standard "Neutron and Gamma-Ray Flux-to-Dose-Rate Factors, ANSI/ANS-6.1.1 (1977). (Published by the American Nuclear Society, 555 N. Kensington Ave., La Grange Park, IL 60525)

ORNL/TM-9801

INTERNAL DISTRIBUTION

1. L. S. Abbott
2. F. S. Alsmiller
3–7. R. G. Alsmiller, Jr.
8–15. J. M. Barnes
16. B. L. Bishop
17–21. J. D. Drischler
22. T. A. Gabriel
23. R. A. Lillie
24. F. C. Maienschein
25. R. W. Peelle
26. RSIC
27. R. T. Santoro
28. A. Zucker
29. P. W. Dickson, Jr. (Consultant)
30. G. H. Golub (Consultant)
31. D. Steiner (Consultant)
32–33. Central Research Library
34. ORNL Y-12 Technical Library Document Reference Section
35–36. Laboratory Records
37. ORNL Patent Office
38. Laboratory Records - RC

EXTERNAL DISTRIBUTION

39. Office of Assistant Manager for Energy Research & Development, DOE-ORO, Oak Ridge, TN 37830

40. Argonne National Laboratory, Library Services Department, 302-CE125, 9700 S. Cass Avenue, Argonne, IL 60439

41. T. W. Armstrong, Science Applications, Inc., PO Box 2807, La Jolla, CA 92038

42. Miguel Awschalom, National Accelerator Laboratory, PO Box 500, Batavia, IL 60510

43. V. S. Barashenkov, Laboratory of Theoretical Physics, Joint Institute for Nuclear Research, Head Post Office, PO Box 79, Moscow, USSR

44. Dr. Elliott Bloom, Stanford Linear Accelerator Center, PO Box 4349, Stanford, CA 94305

45. J. Brau, University of Tennessee, Dept. of Physics, Knoxville, TN 37919

46. Dr. Bruce Brown, Fermi National Accelerator Laboratory, PO Box 500, Batavia, IL 60510

47. Dr. David O. Caldwell, Department of Physics, University of California at Santa Barbara, Santa Barbara, CA 93106

48. Herbert Destaebler, Stanford Linear Accelerator Center, Stanford University, Stanford, CA 94305

49. Dr. Chris Fabjan, CERN, Geneva 23, Switzerland

50. Dr. G. Feldman, Stanford Linear Accelerator Center, Stanford University, Stanford, CA 94305

51. E. Freytag, Deutsches Elektronen-Synchrotron, DESY, 2 Hamburg Dr., Flottbek, Notkesteig 1, W. Germany

52. K. Goebel, Health Physics Group, CERN, 1211 Geneva 23, Switzerland

53. Dr. Herman Grunder, Deputy Director, General Sciences, Lawrence Berkeley Laboratory, Bldg. 50A, Room 4119, 1 Cyclotron Rd., Berkeley, CA 94720

54. H. J. Hargis, University of Tennessee, Department of Physics, Knoxville, TN 37919

55. Frenc Hajnal, Health and Safety Laboratory, U.S. Department of Energy, 376 Hudson St., NY, NY 10014

56. M. Hofert, CERN, 1211 Geneva 23, Switzerland

57. Prof. D. Lal, Tata Institute of Fundamental Research, National Centre of the Government of India for Nuclear Science & Mathematics, Homi Bhabha Rd., Bombay 5, India

58. Lawrence Livermore Laboratory, Technical Information Department, PO box 808, Livermore, CA 94550

59. V. Lebedev, Institute of High Energy Physics, Serpukhov, Moscow Region, USSR

60. Library for Nuclear Science, Massachusetts Institute of Technology at Middleton, Middleton, MA 01949

61. Dr. J. Marks, Accelerator Fusion Research Division, Lawrence Berkeley Laboratory, Bldg. 50, Room 149, 1 Cyclotron Rd., Berkeley, CA 94720

62. A. I. Mincer, University of Maryland, College Park, MD 20742

63. Dr. V. S. Narasimham, Tata Institute of Fundamental Research, Bombay 400 005, India

64. W. R. Nelson, Stanford Linear Accelerator Center, Stanford University, PO Box 4349, Stanford, CA 94305

65. Keran O'Brien, Health and Safety Laboratory, U.S. Department of Energy, 376 Hudson St., NY, NY 10014

66. Dr. T. R. Palfrey, Jr., Department of Physics, Purdue University, West Lafayette, IN 47907

67. Dr. Robert Palmer, Brookhaven National Laboratory, Upton, NY 11973

68. Dr. C. W. Peck, Department of Physics, California Institute of Technology, Pasadena, CA 91109

69. J. Ranft, Karl-Marx University, Physics Section, Linnestrasse 5, 701 Leipzig, W. Germany

70. Dr. Lincoln Reed, Division of High Energy and Nuclear Physics, Department of Energy, Washington, DC 20545

71. Dr. W. Schmidt, Institute of Experimental Nuclear Physics, University of Karlsruhe, 75 Karlsruhe, W. Germany

72. The Secretary, Radiation Group, Lab II, CERN, 1211 Geneva 23, Switzerland

73. B. S. P. Shen, Department of Astronomy, University of Pennsylvania, Philadelphia, PA 19104

74. Stanford Linear Accelerator Center, Attention: Library, PO Box 4349, Stanford, CA 94305

75. Dr. Alan Stevens, Physics Department, Brookhaven National Laboratory, Upton, NY 11973

76. G. R. Stevenson, Radiation Protection Group, Lab II, CERN, 1211 Geneva 23, Switzerland

77. Dr. L. Sulak, Department of Physics, University of Michigan, Ann Arbor, MI 48109

78. R. Tesch, DESY, Hamburg, Notkesteig 1, W. Germany

79. Ralph H. Thomas, University of California, Lawrence Radiation Laboratory, Health Physics Department, Bldg.72, Berkeley, CA 94720

80. V. D. Toneev, Laboratory of Theoretical Physics, Joint Institute for Nuclear Research, Head Post Office, PO Box 79, Moscow, USSR

81. S. C. Tonwar, University of Maryland, College Park, MD 20742

82. W. Turchinetz, Massachusetts Institute of Technology, R26-411, Cambridge, MA 02139

83. Dr. J. Wilczynski, Nuclear Research Center, Karlsruhe, W. Germany

84. G. B. Yodh, University of Maryland, College Park, MD 20742

85. Dr. B. Zeitnitz, Nuclear Research Center, Karlsruhe, W. Germany

86–112. Technical Information Center, PO Box 62, Oak Ridge,TN 37831